Chapter 4

Sensing of ammonia using silver nanoparticles templated on diatom frustules

4.1 Importance of SND in ammonia sensing

In chapter 2, the bioconversion of silver metal ions into silver NPs (Ag-NPs) by using diatom of species *Navicula* containing fucoxanthin, as reducing and stabilizing reagent have been discussed. This is a green biological technique for synthesis of Ag-NPs and is more advantageous than to conventional methods. The process of green synthesis of SND sample was discussed in chapter 2 in details. Monitoring and sensing dissolved ammonia by using this synthesized hybrid nano-material (namely SND) will be discussed in this chapter. The detection of dissolved ammonia, which was based on the color change of reagent in presence of ammonia, was monitored using absorption spectrometer. This material possesses the following significant features. The material

(i) has no need of any other chemical reducing/stabilizing reagent,
(ii) works in ambient environment and has no need of air or oxygen supply,
(iii) requires no external stimulus such as Joule heating or UV illumination for reaction to initiate,
(iv) operates at room temperature,
(v) is eco-friendly,
(vi) has low detection limit,
(vii) has a fast response time,
(viii) is low cost and is abundantly available.

Ammonia is extensively used in many industries like pharmaceutical, explosive, fertilizer, manufacture of plastic, synthetic fiber, paper, refrigeration of large scale foods etc. [1, 2]. Ammonia is also corrosive to human health, creates skin and eye irritation, high concentration causes permanent blindness and lung disorder. It is hazardous to aquatic species and crustaceans even in very low concentrations and more importantly it cannot be converted to less toxic compounds. Moreover, presence of ammonia in human body is an indicator of disorder or disease like liver and kidney collapse, stomach infection by bacteria, cancer, ulcer, diabetes etc. [3-7]. So sensing and monitoring of ammonia is an important issue.

4.2 Structural and compositional characterization of SND and raw diatom frustules

4.2.1 Analysis of X-ray diffraction spectra

To analyze the phases present in the as-prepared samples XRD was employed. The XRD pattern of the samples, namely SND and raw diatom frustules, are shown in figure 4.1. The 2θ values at 38.01º, 44.72º, 64.5º and 77.5º correspond to the diffractions at the crystal planes (111), (200), (220) and (311) when compared with the standard data obtained from JCPDS No.89-3722 for sample SND. The amorphous nature of raw diatom frustules was clearly indicated by from the XRD pattern. The crystalline nature of the SND sample was due to the formation of Ag-NPs and confirmed by sharp and intense peaks obtained in the XRD spectra. The average crystallite size of the prepared NPs attached on diatom cells was also calculated by using Debye-Scherrer formula [8] and found to be 30.35nm corresponding to the high intensity Millar plane (111).

4.2.2 Analysis of SEM-EDX data

The size and morphology of diatom species and attachment of Ag-NPs on these diatom frustules were confirmed by SEM analysis (figure 4.2(a & b)). The size of Ag-NPs ranged from 70nm to 80nm. Analyzing the SEM micrographs and comparing them with diatom identification guides and ecological data sources, it was confirmed that the diatoms belonged to the *Navicula* species [9]. The dimension of the diatom frustules was about 17μm to 20μm in length and about 6μm in width. The EDX was performed (figure 4.2(c)) to analyze the weight %, atomic % and characteristic energy levels of the composition of the as prepared samples and is tabulated in table 4.1. EDX spectrum of the SND sample showed strong characteristic signal of Ag near 3keV. Characteristic peaks observed of Si and O were due to the presence of silica frustules and the peak for C was due to the presence of organic matter.

Table 4.1 EDX compositional analysis of SND sample.

Element	Characteristic Energy levels	Weight (%)	Atomic(%)
C	K	1.35	2.73
O	K	51.23	77.52
Si	K	14.30	12.33
Ag	L	33.11	7.43
Total		100.00	

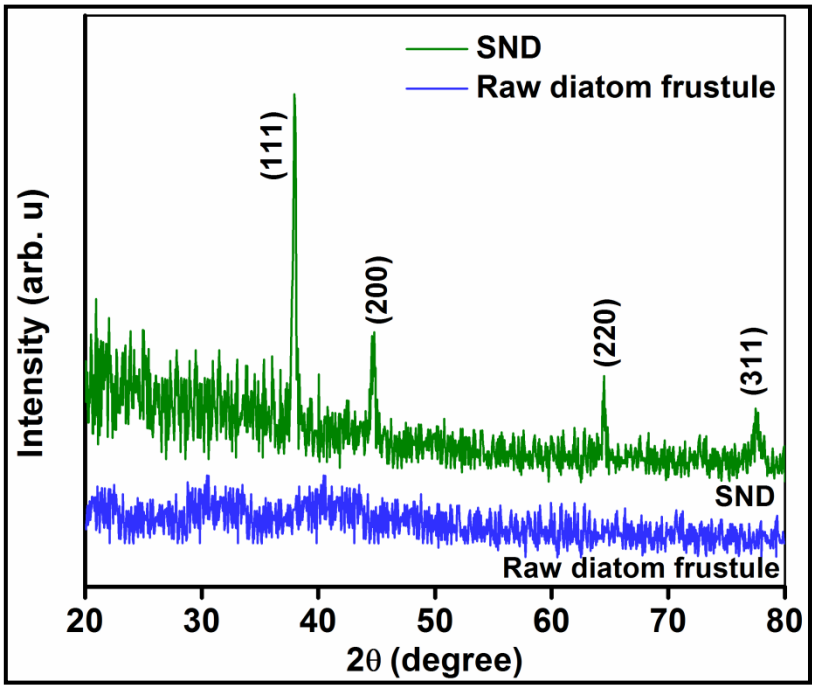

Figure 4.1 XRD spectra of biosynthesized SND sample and raw diatom frustules.

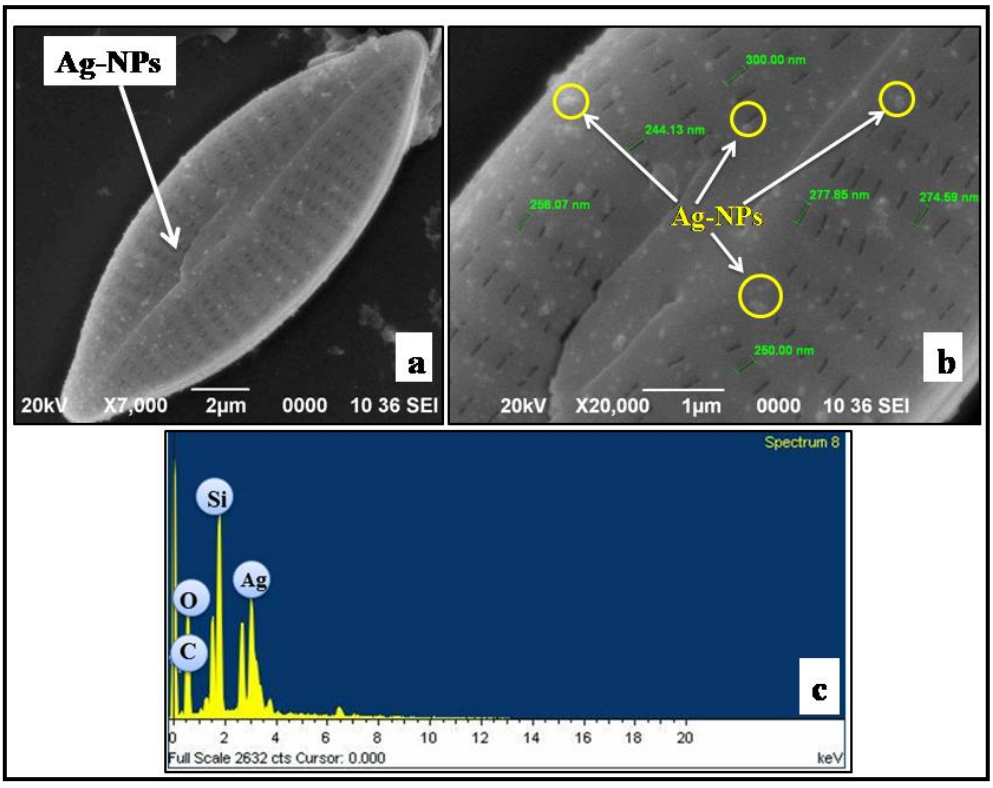

Figure 4.2 (a, b) SEM images of SND showing Ag-NPs formation and (c) EDX spectrum of SND.

4.2.3 Analysis of FTIR spectra of SND and raw diatom frustule

In order to identify the presence of various functional groups in the biomolecules for bio-reduction of Ag^+ ions and efficient stabilization of silver nanoparticles, FTIR measurements were carried out in the wavelength range 4000-400 cm^{-1}. FTIR spectra of dry SND and raw diatom frustules (RD) are shown in figure 4.3. The strong and broad band observed at 3404cm^{-1} for SND and 3445 cm^{-1} for RD sample correspond to the stretching and bending vibration of the -OH groups, basically external silanol groups (Si-OH) of the amorphous silica [8-12]. Bands at 2918cm^{-1} and 2926 cm^{-1} for SND and RD respectively were due to asymmetric stretching modes of $-CH_2$. Again 2853cm^{-1} and 2839 cm^{-1} bands for SND and RD respectively were due to symmetric stretching modes of $-CH_2$ [12]. These symmetric and asymmetric stretching modes of $-CH_2$ were related to the carbon chain of organo-silane molecules in the diatom frustules. Peaks at 1649cm^{-1}, 1634 cm^{-1} for SND and RD respectively were due to the stretching and bending vibration of -OH groups [13]. Peaks at 1376cm^{-1} and 1383 cm^{-1} for SND and RD respectively were due to C=O stretching vibration carboxyl groups present in diatom cells [10, 11]. Peaks at 1029cm^{-1} and 1036 cm^{-1} for SND and RD respectively were due to Si-O-Si asymmetric vibration in the silica composed diatom frustule [13]. The presence of Ag-NPs in the SND was confirmed by the peak at 532cm^{-1} in the FTIR spectrum of SND [14]. From the FTIR analysis, it was concluded that hydroxyl groups (-OH) of fucoxanthin and carbonyl groups (C=O) of proteins had the ability to reduce Ag^+ ions to metallic Ag-NPs and also these functional groups stabilized the medium by preventing agglomeration of NPs [14-16]. The functional groups corresponding to different wavenumber and respective structure are tabulated in Table 4.2.

Table 4.2 Analysis of functional groups of SND and raw diatom frustules.

Wavenumber (cm^{-1})		Functional groups	Corresponding structure
RD	SND		
-	532	-	Ag-Nanoparticles
1036	1029	Silica	Si-O-Si asymmetric stretching vibration
1383	1376	Carbonyl group	C=O stretching vibration
1634	1649	Hydroxyl (-OH) groups	O-H stretching & bending
2839	2853	C-H groups	CH_2 symmetric stretching
2926	2918	C-H groups	CH_2 asymmetric stretching
3445	3404	Silanol groups (-OH group)	Si-OH stretching

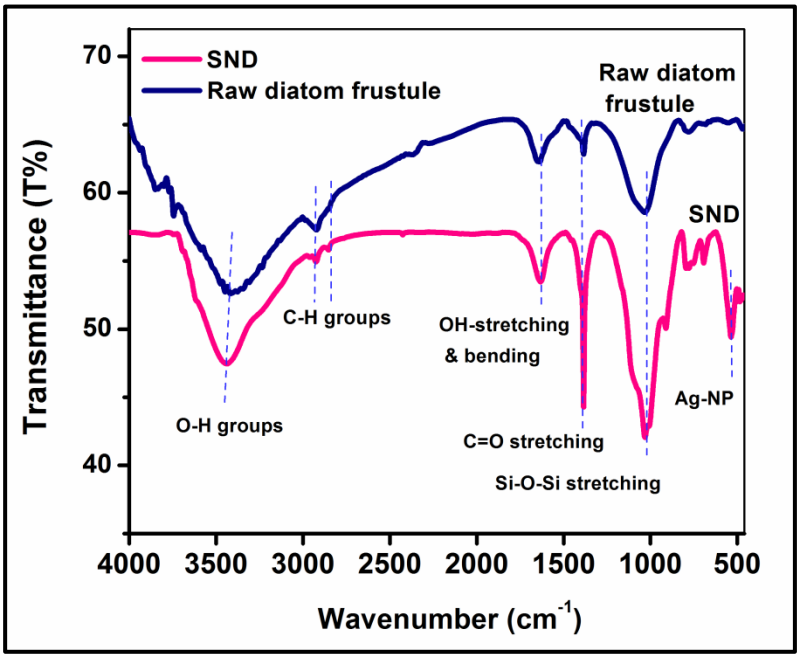

Figure 4.3 FTIR spectra of SND and Raw diatom frustules showing different functional groups.

4.3 Analysis of UV-visible spectra

Figure 4.4 shows the UV-vis spectra of SND and raw diatom frustules. A broad absorption peak ranging from 388nm to 600nm for the Ag-NPs templated on diatom frustules (SND) was observed in the spectrum which was not observed in case of raw diatom frustules. Absorption peak in the UV range from 200nm to 260nm was due to the presence of diatom frustules in both the samples. Broad absorption peak in the range of 388nm-495nm was due to the excitation of free electrons that initiates surface plasmon resonance in the Ag-NPs [17]. Absorption spectra of the sample kept in dark in the second experiment was also studied, but no peak was observed in this range. Thus, light is an essential factor for the synthesis of Ag-NPs by bio-reduction of Ag^+ ion to stable Ag^0 NPs on diatom cells through the involvement of light sensitive bio-molecules in the reaction mechanism. The bio-reduction of silver by organic substances present in raw diatom cells can be understood by equations (1 & 2).

$$AgNO_3 \xrightarrow{H_2O} Ag^+(aq) + NO_3^-(aq) \quad (1)$$

$$Ag^+(aq) + \text{fucoxanthin / hydroxyl group}(-OH) \rightarrow Ag^0(NPs) \quad (2)$$

The mechanism of formation of Ag-NPs in diatom cell under light exposure can be understood in the following way. In the solution, the metallic salt $AgNO_3$ interacts with the cellular organic compounds of phototrophic organisms like diatoms [18]. Diatoms contain photosynthetic pigments namely chlorophyll-a, chlorophyll-c and fucoxanthin. In light harvesting photosystem fucoxanthin plays the most important role and is also responsible for golden brown color of diatoms [19, 20]. Fucoxanthin belongs to the Xanthophyll group and contains hydroxyl, carbonyl, epoxy, carboxyl etc. oxygenic functional groups [21]. Though it is not possible for pure fucoxanthin to stabilize and control the size of NPs, the hydroxyl group (-OH) present in the fucoxanthin structure makes it a reducing agent in conjunction with protein and some other biomolecules present in the organic part of the diatom cell in the presence of light. Organic compounds, carbohydrates, proteins and Silaffins are the main agents for the reduction of metal ions to stable metal NPs through oxidation of hydroxyl groups (-OH) to carbonyl groups in silver NPs biosynthesis process [18, 21]. Silaffin is a class of heavily post-translationally modified protein. They possess silica deposition at ambient temperature and pressure and are also active agent in the synthesis of metal NPs and silica NPs in diatom cells [22]. Figure 4.5 shows a schematic diagram of the formation of Ag-NPs through slow nucleation process using fucoxanthin containing diatom frustules.

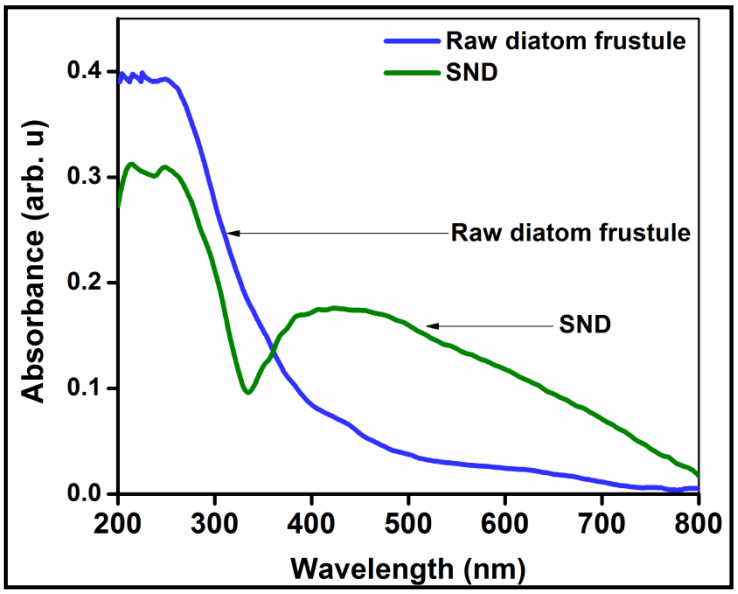

Figure 4.4 UV-vis absorption spectra of as-synthesized SNDs and raw diatom frustules.

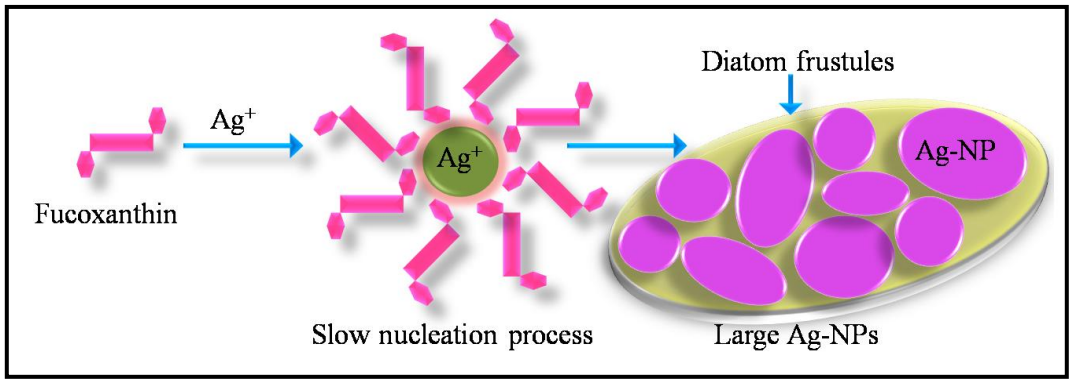

Figure 4.5 Schematic showing the formation of Ag-NPs through slow nucleation process using fucoxanthin containing diatom frustules.

4.4 Sensing of ammonia using SND

Sensing behavior of SND can be explained on the basis of observations from the UV-vis absorption spectra. For this purpose different concentration of ammonia was fixed with equal amount of SND sample and their UV-vis absorption spectra was monitored. It was observed that with increasing ammonia concentration the purple color of SND changed to light yellow color having blue shift in the absorption peak which is shown in figure 4.6. Figure 4.6 (a) shows the absorbance spectra for 0, 20, 40, 60, 80 and 100ppm concentration ammonia solution having equal amount of the as prepared SND sample. A broad absorption peak was observed at zero concentration having maximum absorption peak position at 570nm. As the ammonia concentration was increased, intensity of this peak gradually decreased and the peak shifted from 570nm at zero concentration to another position at 457nm at 100ppm concentration of ammonia. NPs were formed by nucleation and growth process in which nucleation to growth rate ratio gave the final size of the NPs. Slow nucleation rate gave growth to large polydisperse size nanoparticles and fast nucleation rate produced small size NPs [1]. Figure 4.7 shows schematic of sensing mechanism of ammonia through the synthesis of Ag-NPs using diatom frustules by fast nucleation process.

From experimental observations, it was found that with increase in ammonia concentration the initial broad absorption peak disappear gradually and the newly formed peaks get blue shifted. This was due to the fact that Ag-NPs formation in the absence of ammonia was slow and the size of the NPs was larger than that would have been in the presence of ammonia in the growth process. With increase in the ammonia concentration, formation of isolated NPs increased, which was indicated by the enhancement of blue shifted peaks. The blue shift in the peaks indicated that the NPs formed were smaller in size. Shifting of absorption peak was due to the combined effect of change in inter-particle spacing and dielectric constant of the surrounding medium [5]. The bio-reduction of silver by diatom cells in the presence of ammonia is explained by equations (3, 4).

$$Ag^{+}(aq) + 2NH_3 \Leftrightarrow [Ag(NH_3)_2]^{+}(aq) \quad (3)$$

$$[Ag(NH_3)]^{+}(aq) + \text{Fucoxanthin / hydroxyl group}(-OH) \rightarrow Ag^{0} + \text{other products} \quad (4)$$

The shifting of 570nm peak was due to the complexation of ammonia with Ag^{+} ions. Ammonia plays an important role in the reduction of Ag^{+} ions by organic substances. When we added ammonia solution to our prepared sample of silver NPs attached to diatom cells, $[Ag(NH_3)_2]^{+}$

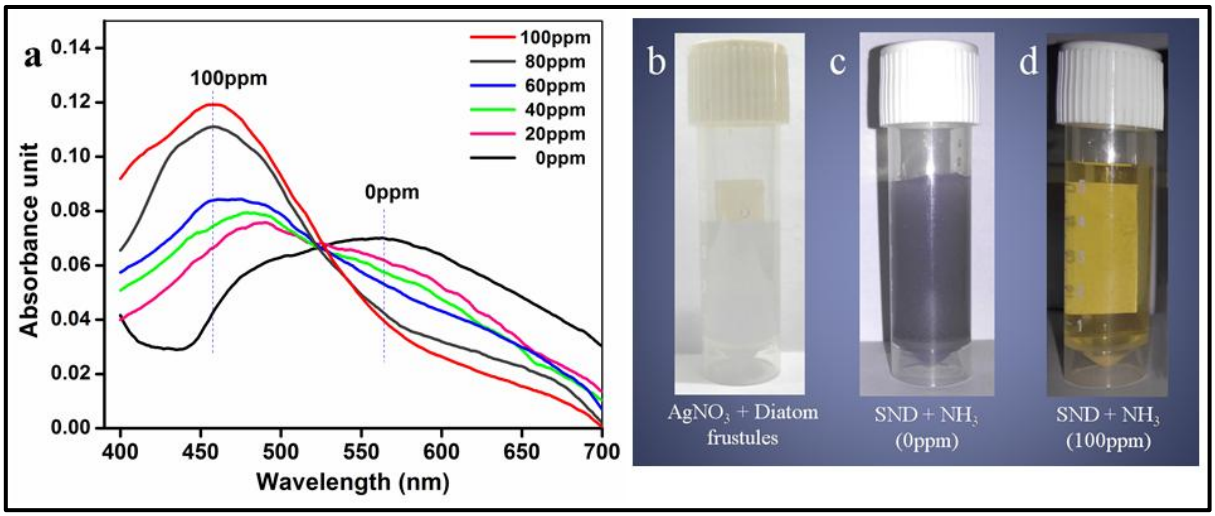

Figure 4.6 (a) UV-vis absorption spectra of SND sample exposed to 0, 20, 40, 60, 80 and 100ppm concentrations of ammonia solution, (b) $AgNO_3$ solution and diatom frustule (control), SND in (c) 0ppm and (d) 100ppm NH_3 concentration.

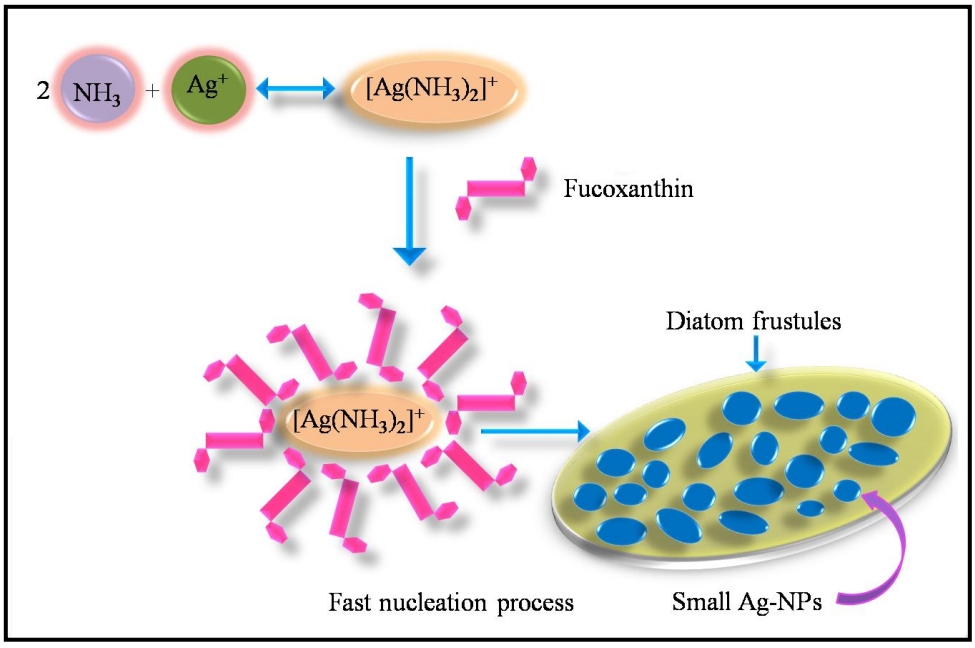

Figure 4.7 Schematic of sensing mechanism of ammonia through the synthesis of Ag-NPs using diatom frustules by fast nucleation process.

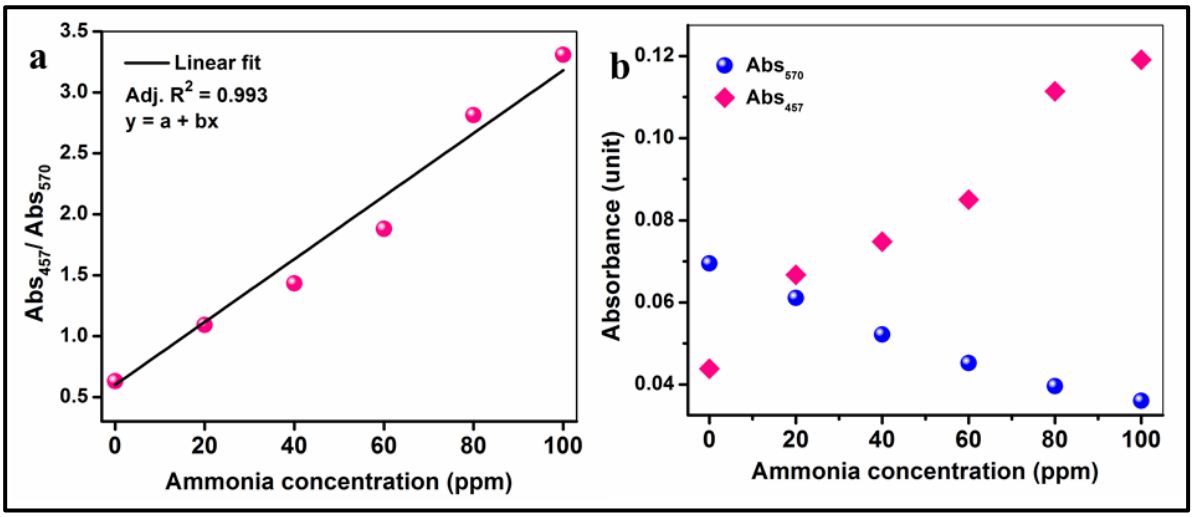

Figure 4.8 (a) Absorbance ratio at 457nm and 570nm which displays a linear relationship as a function of ammonia concentration (0ppm to100ppm) with a correlation factor R^2 equal to 0.993 and (b) Plot of absorbance 457nm and 570nm vs ammonia concentration.

complex was formed due to the reaction between ammonia and Ag^+ ions, which reduced the reduction potential of Ag^+ ions and hence decreased the nucleation rate and growth of NPs. In presence of ammonia there is always a competition between organic substances and ammonia to react with Ag^+[23] and ammonia has strong affinity towards Ag^+ and to form $[Ag(NH_3)_2]^+$. When ammonia concentration was increased, the number of formation of $[Ag(NH_3)_2]^+$ complex was also increased. With the increase in number of $[Ag(NH_3)_2]^+$ complexes, surface charge of the particles also increased and caused repulsion between the particles. So water content increased in the surrounding of the particles that resulted in small isolated particles [4]. The blue shifting of the spectra and increase in intensity with increase in ammonia concentration, in this observation, was due to the formation of more number of isolated and smaller nano-complexes caused by Coulombic repulsion. The organic substances present in the diatoms finally reduced the $[Ag(NH_3)_2]^+$ complex into metallic silver nanoparticles (Ag^0).

For the design of ammonia optical sensor, it was necessary to choose two specific wavelengths at which the variation of intensities of absorption in the UV-Vis spectra was maximum, instead of considering the entire spectrum range, during the sensing experiment. For this reason, the absorption ratio (Abs_{457}/Abs_{570}) and absorption intensity change as a function of ammonia concentration at wavelengths 570nm and 457nm are plotted in figure 4.8 (a & b) respectively. A linear relationship having correlation factor R^2 equals to 0.993 was observed from the absorption ratio versus ammonia concentration plot which depicted that with increase in ammonia concentration the absorption ratio increased linearly. From these results we conclude that SNDs are highly capable of detection of lower concentration ammonia dissolved in solution (up to 100ppm in our study) and can act as a reliable optical sensor for ammonia sensing.

4.5 Conclusions

In this chapter, a very simple and highly effective photo-induced bio-reduction process of Ag-NPs incorporated in with diatom cells at room temperature under basic conditions was presented. The interaction of diatoms with aqueous salt $AgNO_3$ promoted the formation of NPs in the presence of light. No other external reducing/stabilizing agents were used in this method and only fucoxanthin present in the diatom cells, independent of diatom species, was responsible for the bio-reduction of Ag-NPs in the presence of day light. Presence of protein components in the diatom cells which act as stabilizing agent for Ag-NPs, was revealed by FTIR analysis. This green bio-synthesis of NPs using diatom cells is eco-friendly, worthwhile, energy efficient, harmless to human health, effective, low-cost and has benefits since it leads to large-scale production of NPs easily. Further these biologically synthesized metal NPs show efficient sensing behavior of dissolved ammonia in the 0-100ppm range at ambient temperature.

[Note: This work is published in the journal "Sensing and Bio-Sensing Research"

Chetia, L., Kalita, D. and Ahmed, G. A. Synthesis of Ag nanoparticles using diatom cells for ammonia sensing. *Sensing and Bio-Sensing Research*, 16:55-61, 2017. DOI: 10.1016/j.sbsr.2017.11.004.]

References

[1] Edison, T. N. J. I., Atchudan, R. and Lee, Y. R. Optical Sensor for Dissolved Ammonia Through the Green Synthesis of Silver Nanoparticles by Fruit Extract of Terminalia chebula. *The Journal of Cluster Science*, 27: 683-690, 2016. DOI:10.1007/s10876-016-0972-4.

[2] Cannilla, C., Bonura, G., Frusteri, F., Spadaro, D., Trocino, S. and Neri, G. Development of an ammonia sensor based on silver nanoparticles in a poly-methacrylic acid matrix. *Journal of Materials Chemistry C*, 2:5778, 2014. DOI:10.1039/c4tc00515e.

[3] Pandey, S., Goswami, G. K. and Nanda, K. K. Green synthesis of polysaccharide/gold nanoparticle nanocomposite: An efficient ammonia sensor. *Carbohydrate Polymers*, 94:229-234, 2013. DOI:10.1016/j.carbpol.2013.01.009.

[4] Dubas, S. T. and Pimpan, V. Green synthesis of silver nanoparticles for ammonia sensing. *Talanta*, 76:29-3, 2008. DOI:10.1016/j.talanta.2008.01.062.

[5] Pandey, S., Goswami, G. K. and Nanda, K. K. Green synthesis of biopolymer–silver nanoparticle nanocomposite: An optical sensor for ammonia detection. *International Journal of Biological Macromolecules*, 51:583-589, 2012. DOI: 10.1016/j.ijbiomac.2012.06.033.

[6] Tadi, K. K., Pal, S. and Narayanan, T. N. Fluorographene based Ultrasensitive Ammonia Sensor, *Scientific Reports*, 6:25221, 2016. DOI: 10.1038/srep25221.

[7] Das, T., Pramanik, A. and Haldar, D. On-line Ammonia Sensor and Invisible Security Ink by Fluorescent Zwitterionic Spirocyclic Meisenheimer Complex. *Scientific Reports*, 7:40465, 2017. DOI: 10.1038/srep40465

[8] Chetia, L., Kalita, D. and Ahmed, G. A. Enhanced photocatalytic degradation by diatom templated mixed phase titania nanostructure, *Journal of Photochemistry and Photobiology A: Chemistry*, 338:134-145, 2017. DOI:10.1016/j.jphotochem.2017.01.035.

[9] Taylor, J. C., Harding, W. R. and Archibald, C. G. M. An Illustrated Guide to Some Common Diatom Species from South Africa, Report to the Water Research Commission. Technical Report No. TT 282/07, Water Research Commission, Private Bag X03, Gezina 0031, Pretoria, South Africa, 2007.

[10] Zhang, J., Ding, T., Zhang, Z., Xu, L. and Zhang, C. Enhanced Adsorption of Trivalent Arsenic from Water by Functionalized Diatom Silica Shells. *PLoS ONE*, 10(4):e0123395, 2015. DOI:10.1371/journal.pone.0123395.

[11] Xia, S., Gao, B., Li, A., Xiong, J., Ao, Z. and Zhang, C. Preliminary Characterization, Antioxidant Properties and Production of Chrysolaminarin from Marine Diatom Odontellaaurita. *Marine Drugs*,12:4883-4897, 2014. DOI:10.3390/md12094883.

[12] Sprynskyy, M., Kowalkowski, T., Tutu, H., Cukrowska, E. M. and Buszewski, B. Ionic liquid modified diatomite as a new effective adsorbent foruranium ions removal from aqueous solution. *Colloids and Surfaces A: Physicochemical and Engineering Aspects*, 465:159-167, 2015. DOI: 10.1016/j.colsurfa.2014.10.042.

[13] Stuart, B. *Infrared Spectroscopy: Fundamentals and Applications*, John Wiley & Sons, 2004. ISBN: 978-0-470-85428-0.

[14] Panigrahi, T. Synthesis and characterization of silver nanoparticles using leaf extract of Azadirachta indica. Master's thesis, Department of life science, National Institute of Technology, Rourkela-769008, Orissa, India, 2013.

[15] Phanjom, P. and Ahmed, G., Biosynthesis of Silver Nanoparticles by Aspergillus oryzae (MTCC No. 1846) and Its Characterizations. *Nanoscience and Nanotechnology*, 5(1):14-21, 2015. DOI:10.5923/j.nn.20150501.03.

[16] Danwanichakul, P., Suwatthanarak, T., Suwanvisith, C. and Danwanichakul, D. The Role of Ammonia in Synthesis of Silver Nanoparticles in Skim Natural Rubber Latex. *Journal of Nanoscience*, 2016:7258313, 2016. DOI: 10.1155/2016/7258313.

[17] Fayaz, A. M., Balaji, K., Girilal, M., Yadav, R., Kalaichelvan, P. T. and Venketesan, R. Biogenic synthesis of silver nanoparticles and their synergistic effect with antibiotics: a study against gram-positive and gram-negative bacteria. *Nanomedicine: Nanotechnology, Biology and Medicine*, 6:103-109, 2010. DOI:10.1016/j.nano.2009.04.006.

[18] Schrofel, A., Kratosova, G., Bohunicka, M., Dobrocka, E. and Vavra, I. Biosynthesis of gold nanoparticles using diatoms-silica gold and EPS-gold bionanocomposite formation. *The Journal of Nanoparticle Research*, 13:3207-3216, 2011. DOI:10.1007/s11051-011-0221-6.

[19] Rajauria, G., and Ghannam, N. A. Isolation and Partial Characterization of Bioactive Fucoxanthin from Himanthalia elongata Brown Seaweed: A TLC-Based Approach,

International Journal of Analytical Chemistry, 2013:802573, 2013. DOI: 10.1155/2013/802573.

[20] Yan, X., Chuda, Y., Suzuki, M. and Nagata, T. Fucoxanthin as the Major Antioxidant in Hijikia fusiformis, a Common Edible Seaweed. *Bioscience, Biotechnology, and Biochemistry*, 63(3):605-607, 2014. DOI: 10.1271/bbb.63.605.

[21] Jena, J., Pradhan, N., Dash, B. P., Panda, P. K. and Mishra, B. K. Pigment mediated biogenic synthesis of silver nanoparticles using diatom Amphora sp. and its antimicrobial activity.*Journal of Saudi Chemical Society*, 19(6):661-666, 2014. DOI: 10.1016/j.jscs.2014.06.005

[22] Lechner, C. C. and Becker, C. F. W. Silaffins in Silica Biomineralization and Biomimetic Silica Precipitation. *Marine Drugs*, 13:5297-5333, 2015. DOI:10.3390/md13085297.

[23] Khan, Z., Hussain, J. I., Kumar, S., Hashmi, A. A. and Malik, M. A. Silver Nanoparticles: Green Route, Stability and Effect of Additives. *Journal of Biomaterials and Nanobiotechnology*, 2:390-399, 2011. DOI:10.4236/jbnb.2011.24048.